Unified and stable scattering matrix formalism for acoustic waves in piezoelectric stacks

Victor Y. Zhang, Vincent Laude

Unified and stable scattering matrix formalism for acoustic waves in piezoelectric stacks

Cite as: J. Appl. Phys. **104**, 064916 (2008); https://doi.org/10.1063/1.2978219
Submitted: 10 March 2008 • Accepted: 15 July 2008 • Published Online: 26 September 2008

Victor Y. Zhang and Vincent Laude

Unified and stable scattering matrix formalism for acoustic waves in piezoelectric stacks

Victor Y. Zhang[1,a)] and Vincent Laude[2,b)]
[1]*Institut d'Electronique, de Microélectronique, et de Nanotechnologie (IEMN), UMR CNRS, 8520 Av. Poincaré, BP 60069, 59652 Villeneuve d'Ascq Cedex, France*
[2]*Institut FEMTO-ST, UMR CNRS 6174 (CNRS, UFC, ENSMM, UTBM), 32 Avenue de l'Observatoire, 25044 Besançon Cedex, France*

(Received 10 March 2008; accepted 15 July 2008; published online 26 September 2008)

This paper presents a unified and full *scattering matrix* (**s**-matrix) formalism for modeling of acoustic waves in piezoelectric multilayered structures. A stable recursive algorithm is derived for computation of the *total* **s**-matrix of a stack in terms of the *interface* **s**-matrix, both referring to the eigenmode amplitudes. The derivation is direct and succinct, the deduced expressions of the **s**-matrix are terse and concise, and the recursion algorithm is efficient and convenient for implementation. The total **s**-matrix recursion scheme differs from the previously published partial matrix algorithms in that the recursions are conducted once for all independent of the stack boundary conditions and so the same results apply for any post-specified boundary condition. Numerical examples are given to show its numerical features that are superior to other currently used matrix formalisms, such as unconditional stability for both large and small thicknesses, being pole-free and branch point-sensitive, constant mean magnitude with stable phase, involving only dimensionless elements. © *2008 American Institute of Physics*.
[DOI: 10.1063/1.2978219]

I. INTRODUCTION

Investigations of wave propagation and interaction with various materials of various geometries are required in many scientific fields and high-tech engineering applications. Many advanced technological devices employing direct electromechanical transduction require piezoelectric materials that are necessarily anisotropic. Even so, some specific properties, unavailable in homogeneous media have to be acquired by means of composites stacking different materials together. Modeling of wave propagation in these structures is often a problem complicated enough to be out of reach of analytical calculations. A variety of matrix formalisms were developed during the past decades for numerical simulations. Among the most typical and representative models, the transfer **T**-matrix[1–3] is certainly the most widely well-known. Unfortunately, the intuitive and easy-to-process **T**-matrix model was rapidly recognized to suffer from numerical instability at the high frequency regime, as measured by the frequency-thickness product *fh*. To circumvent the numerical instability of the classical **T**-matrix, which becomes a serious obstacle in analyzing miniaturized devices operating at high frequencies, a variety of different matrices have been proposed for wave modeling. The last to date is the hybrid **H**-matrix mixing the compliance/stiffness.[4] A veritable breakthrough advance in eliminating the harmful numerical instability within the realm of matrix models for acoustic waves in piezoelectric heterostructures originated from the impedance **Z**-matrix,[5–7] comprising its direct variant compliance/stiffness **K**-matrix,[8,9] and some scattering **s**-matrix related approaches[10–14] that are in reality partial **s**-matrix formulas. In order for readers to have a quick reference and a clear comparison at a glance, in Table I we summarize the regular and modified definitions of the aforementioned matrices, their mostly known variants, all in relation to the physical quantities, along with their important properties which we will analyze later in more detail. In effect, their differences are very subtle. Depending on the journals in which they appear and on the scientific communities who employ them, often the same matrix was presented in different forms and sometimes the same matrix name was attributed to different physical definitions. The **H**-matrix recursion presented in Ref. 4 was conducted indirectly without using the full **H**-matrix. Similar is the quarter **Z**-matrix recursion presented in Ref. 6 for nonpiezoelectric media and in Ref. 7 for piezoelectric media. In the book of Kennett,[10] which treats the seismic wave propagation in stratified nonpiezoelectric media, only the partial matrix recursions were implemented in terms of the reflection and transmission matrices. Although the **s**-matrix idea was largely developed, the term "scattering matrix" never appears throughout the book. The first stable recursion proposed by Pastureaud *et al.*[12] for analyzing acoustic waves in piezoelectric stacks is, in fact, a quarter **s**-matrix formalism based on the reflection **R**-matrix. Very similar to the work of Kennett,[10] a half matrix recursion was implemented by Tan[13] for nonpiezoelectric media, again using a submatrix-based indirect recursion. Although later all of the four submatrices of a full **s**-matrix for piezoelectric media were also provided,[15] they appeared under the name of *reflection* and *transmission* matrices and were derived as the result of a somewhat cumbersome procedure. In both papers[12,13] entitled scattering matrix method or formalism, neither the **s**-matrix was clearly defined as an entity nor the recursive algorithms were derived in terms of the **s**-matrix itself. Only some submatrices of the **s**-matrix were given

a)Electronic mail: victor.zhang@iemn.univ-lille1.fr.
b)Electronic mail: vincent.laude@femto-st.fr.

TABLE I. Definition and properties of various matrices. Note: to facilitate the understanding and comparison, we have used the same symbols to denote the same physical variables defining the matrices even if they were originally presented with different symbols: **t** and **v**, generalized (normal) stress and velocity vectors; **w** and **u**, generalized deformation and displacement vectors; y_x, amplitude vector of the direct ($x=D$) and inverse ($x=I$) modes; $\mathbf{v}=i\omega\mathbf{u}$, $\mathbf{w}=-ik\mathbf{u}$ for harmonic regimes assumed in the current studies; ω, circular frequency; and k, wavenumber. The superscripts + and − denote the values of a vector at the top and bottom of a layer or a stack, respectively. To avoid confusion, we adopted the symbols **X** to denote the layer stress vector (in place of **T** already reserved by the transfer matrix) and **W** to denote the layer deformation vector (in place of **S** already reserved by the scattering matrix).

Nomination, symbol, and field variables	*Impedance* **Z**: $\mathbf{X}\equiv[\mathbf{t}^-;\mathbf{t}^+]$, $\mathbf{V}\equiv[\mathbf{v}^-;\mathbf{v}^+]$	*Stiffness* **K**: $\mathbf{X}\equiv[\mathbf{t}^-;\mathbf{t}^+]$, $\mathbf{W}\equiv[\mathbf{w}^-;\mathbf{w}^+]$, $\mathbf{U}\equiv[\mathbf{u}^-;\mathbf{u}^+]$	*Transfer* **T** of state vector[a] $\boldsymbol{\tau}\equiv[\mathbf{t};\mathbf{v}]$	*Hybrid* **H** of impedance-admittance of Tan[b] $a\equiv[\mathbf{t}^-;\mathbf{v}^+]$, $\mathbf{b}\equiv[\mathbf{v}^-;\mathbf{t}^+]$	*Scattering* **S**: mode amplitudes $\mathbf{y}_{\text{out}}\equiv[\mathbf{y}_I^{(n)};\mathbf{y}_D^{(n+1)}]$,[c] $\mathbf{y}_{\text{in}}\equiv[\mathbf{y}_D^{(n)};\mathbf{y}_I^{(n+1)}]$
Basic definition	$\mathbf{X}\equiv[\mathbf{Z}]\mathbf{V}$	$\mathbf{X}\equiv[\mathbf{K}]\mathbf{W}$	$\boldsymbol{\tau}^+\equiv[\mathbf{T}]\boldsymbol{\tau}^-$	$\mathbf{a}\equiv[\mathbf{H}]\mathbf{b}$	$\mathbf{y}_{\text{out}}\equiv[\mathbf{S}]\mathbf{y}_{\text{in}}$
Variants of the same family	$\mathbf{X}\equiv[\mathbf{t}^+;\mathbf{t}^-]$, $\mathbf{V}\equiv[\mathbf{v}^+;\mathbf{v}^-]$; or **Z** inverse: *Admittance* $\mathbf{Y}\equiv\mathbf{Z}^{-1}$	*Stiffness* $\mathbf{K}'$ of Rokhlin[d]: $\mathbf{X}\equiv[\mathbf{K}']\mathbf{U}$; or **K** inverse: *Compliance* $\mathbf{C}\equiv\mathbf{K}^{-1}$	According to arrangement of $\boldsymbol{\tau}$: $\boldsymbol{\tau}[\mathbf{v};\mathbf{t}]$ $\boldsymbol{\tau}\equiv[\mathbf{t};\mathbf{u}]$ $\boldsymbol{\tau}\equiv[\mathbf{u};\mathbf{t}];\ldots$	Rokhlin type compliance-stiffness of Tan[e], $\mathbf{a}\equiv[\mathbf{u}^-;\mathbf{t}^+]$ $\mathbf{b}\equiv[\mathbf{t}^-;\mathbf{u}^+]$	$\mathbf{y}_{\text{out}}\equiv[\mathbf{y}_D^{(n+1)};\mathbf{y}_I^{(n)}]$, $\mathbf{y}_{\text{in}}\equiv[\mathbf{y}_I^{(n+1)};\mathbf{y}_D^{(n)}]$
Poles/SSBW	With poles No SSBW	With poles No SSBW	No poles No SSBW	(Unknown)	No poles SSBW-sensitive
For $fh\to\infty$	Stable diagonal matrix	Stable diagonal matrix	Singular[f] unstable	Stable diagonal matrix	Stable matrix with (1,1) or (2,2) element
For $fh\to 0$	Singular[g] unstable	Singular[g] unstable	Stable identity matrix	Stable antidiagonal matrix of unitary elements	Stable full matrix
Matrix elements	Homogeneous	Homogeneous	Heterogeneous	Heterogeneous	Dimensionless
Physical meanings of submatrices	Four impedance submatrices	Four stiffness submatrices	1 impedance 1 admittance 2 transfer	Similar to **T**	2 **T**ransmission and 2 **R**eflection submatrices

[a]References 2 and 20.
[b]Reference 15.
[c]n denotes the interface number.
[d]References 8 and 9.
[e]Reference 4.
[f]To invert a matrix containing some zero columns.
[g]To invert a matrix containing some identical columns.

instead, and they were "scattered" in different equations and in the various expressions.

Among many stable matrix formalisms available now, the scattering matrix-based modeling is the only one that considers the eigenmode amplitudes as unknown variables instead of the physical field quantities.[12] Herein, we use the words "matrix formalism" to designate both the basic matrix relative to a single layer, defined after a specific physical signification, and the associated recursive algorithm necessary for dealing with a stack of several layers. The usefulness and deficiencies of various algorithms and their variants were lengthily discussed in a very recent paper,[15] along with their computational efficiency and numerical stability across large and small thicknesses quantitatively compared. Obvious similarities and subtle differences among the aforementioned matrix formalisms, their respective rationale, advantages, and disadvantages, as well as their interrelationships, were also addressed. So the present paper does not intend to attempt an overall comment and comparison or to claim a complete synthesis. Instead, we aim to provide a natural definition and a direct derivation of the **s**-matrix formalism because we consider that the **s**-matrix published up to now dealing with acoustical waves[10–14] has not been introduced in a way as direct and not presented in a form as concise as it should be, compared with the **s**-matrix used by microwave electronic engineers[16] or by researchers in other fields.[17,18] In effect, they were derived in several variant forms, expressed with different terminologies and with different notations, often given in the partial form, and thus confused with the reflection **R**-matrix. We believe that this is certainly a reason why the numerical superiority of the **s**-matrix formalism is, to the best of our knowledge, not sufficiently illustrious and influential, and especially not fully exploited for modeling of acoustic waves in piezoelectric multilayered structures. More significantly, any partial **s**-matrix approach has to incorporate the stack *boundary conditions* (BCs) into the recursive algo-

rithm itself by specifying them at the outset of the recursion. Due to incorporation of a specific BC into the partial **s**-matrix recursion at one side of the stack, the recursion has to be repeated if a different BC is needed to be considered for the same stack. In a number of situations, it is indeed useful to specify independent BC on both sides of a composite layered plate. For instance, wave generation and propagation in a plate with corrugations or patterned electrodes on its outer surfaces can be adequately described by combining plane wave analysis for the homogeneous stack and finite element analysis for the heterogeneous part of the problem, as discussed by Reinhardt *et al.*[19] In Ref. 19, a somewhat cumbersome method was employed to obtain the full Green's functions of the composite plate, based on the **R**-matrix algorithm, which involves varying the BC on one side to obtain block matrices of the Green's functions. The **s**-matrix algorithm presented here would give the required Green's functions at no additional expense. To remedy the deficiencies of the partial **s**-matrix recursion schemes, we offer here a veritable full **s**-matrix formalism which, similar to that used for **K**-matrix,[8,9] differs significantly from the previously published **R**-matrix,[12] or quarter- and half-matrix formalisms.[10,13,15]

This paper is organized as follows. The basic **s**-matrix for an elementary black-box containing a layer and an interface is first introduced as a linear relation between mode amplitudes. A recursive algorithm is then developed to formulate the **s**-matrix of a stack containing a finite number of boxes in terms of the **s**-matrix of the last single box and the **s**-matrix of the stack without the last box. Finally, the basic **s**-matrix is expressed by the product of the *layer scatterer* and the *interface scattering matrix*. The stack BCs are introduced in terms of two surface impedance matrices of the external media surrounding the stack. The same **s**-matrix recursion results are combined with various stack BCs to establish a corresponding homogeneous system. Setting to zero the system determinant yields the BC-dependent proper modes. Examples are provided to demonstrate particular numerical features of the **s**-matrix, such as pole-free, branch point-sensitive, constant mean magnitude with stable phase, and involving only dimensionless elements, in addition to its stability in both high and low *fh* regimes.

II. BASIC S-MATRIX AND RECURSIVE ALGORITHM FOR A STACK

To begin with, we consider a black-box containing a single layer n of thickness h_n and an interface separating it with the next layer $n+1$, as illustrated in Fig. 1. The symbols $\mathbf{y}_{xn}^{\pm}$ $(x=D,I)$ denote the wave amplitudes of the *direct* (D) and *inverse* (I) modes at the top $(-)$ and bottom $(+)$ surface of the layer n. The sense of direct refers to the positive x_2 direction. We introduce an eight-dimensional matrix $\mathbf{S}^n$ to express the output modes' amplitudes in terms of the input ones. The terms input and output refer to the box. Thus the matrix $\mathbf{S}^n$, which is called *generalized interface scattering matrix* (GISM), is defined for the box n by

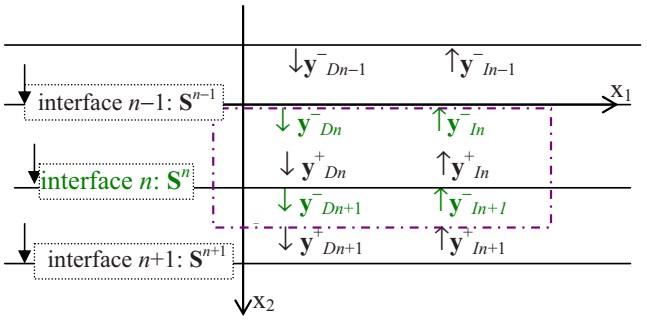

FIG. 1. (Color online) Schematic of a box containing a layer and an interface separating it with the next layer along with notations for the mode amplitudes used in defining the GISM $\mathbf{S}^n$ of the box n.

$$\begin{bmatrix} \mathbf{y}^-_{In} \\ \mathbf{y}^-_{Dn+1} \end{bmatrix} \equiv \begin{bmatrix} \mathbf{S}^n_{11} & \mathbf{S}^n_{12} \\ \mathbf{S}^n_{21} & \mathbf{S}^n_{22} \end{bmatrix} \begin{bmatrix} \mathbf{y}^-_{Dn} \\ \mathbf{y}^-_{In+1} \end{bmatrix}, \tag{1}$$

where the layer index n can take any integer value (positive, negative, or zero). This definition is totally coherent with the well-known *s*-parameter matrix of a two-port network widely used in microwave circuit analysis.[16] The GISM, $\mathbf{S}^{n+1}$ of the next box $n+1$ is defined in the same way and yields from Eq. (1) upon substituting n with $n+1$. The *generalized total scattering matrix* (GTSM) of the system containing two boxes n and $n+1$, noted as $\mathbf{s}^{n;2}$, is similarly defined by

$$\begin{bmatrix} \mathbf{y}^-_{In} \\ \mathbf{y}^-_{Dn+2} \end{bmatrix} \equiv \begin{bmatrix} \mathbf{s}^{n;2}_{11} & s^{n;2}_{12} \\ \mathbf{s}^{n;2}_{21} & s^{n;2}_{22} \end{bmatrix} \begin{bmatrix} \mathbf{y}^-_{Dn} \\ \mathbf{y}^-_{In+2} \end{bmatrix}. \tag{2}$$

As usual, we assume a perfect contact at the interface between any two adjacent layers in the multilayered structure (called stack) and no interface is metallized. This state vector continuity allows us to express the matrix $\mathbf{s}^{n;2}$ in terms of the matrices $\mathbf{S}^n$ and $\mathbf{S}^{n+1}$ once the wave amplitudes $\mathbf{y}^-_{Dn+1}$ and $\mathbf{y}^-_{In+1}$ at the interface $n+1$ are eliminated. We write the final results in the following form:

$$\mathbf{s}^{n;2}_{11} = \mathbf{S}^n_{11} + \mathbf{S}^n_{12}[\mathbf{I} - \mathbf{S}^{n+1}_{11}\mathbf{S}^n_{22}]^{-1}\mathbf{S}^{n+1}_{11}\mathbf{S}^n_{21}, \tag{3a}$$

$$\mathbf{s}^{n;2}_{12} = \mathbf{S}^n_{12}[\mathbf{I} - \mathbf{S}^{n+1}_{11}\mathbf{S}^n_{22}]^{-1}\mathbf{S}^{n+1}_{12}, \tag{3b}$$

$$\mathbf{s}^{n;2}_{21} = \mathbf{S}^{n+1}_{21}[\mathbf{I} - \mathbf{S}^n_{22}\mathbf{S}^{n+1}_{11}]^{-1}\mathbf{S}^n_{21}, \tag{3c}$$

$$\mathbf{s}^{n;2}_{22} = \mathbf{S}^{n+1}_{22} + \mathbf{S}^{n+1}_{21}\mathbf{S}^n_{22}[\mathbf{I} - \mathbf{S}^{n+1}_{11}\mathbf{S}^n_{22}]^{-1}\mathbf{S}^{n+1}_{12}. \tag{3d}$$

By substituting $\mathbf{S}^n_{ij}$ with $\mathbf{s}^{n;1}_{ij}$ and keeping $\mathbf{S}^{n+1}_{ij}$ unchanged in Eqs. (3a)–(3d), we obtain a recursive algorithm for calculating $\mathbf{s}^{n;2}$ from $\mathbf{s}^{n;1} \equiv \mathbf{S}^n$ and $\mathbf{S}^{n+1}$ as follows:

$$\mathbf{s}^{n;2}_{11} = \mathbf{s}^{n;1}_{11} + \mathbf{s}^{n;1}_{12}[\mathbf{I} - \mathbf{S}^{n+1}_{11}\mathbf{s}^{n;1}_{22}]^{-1}\mathbf{S}^{n+1}_{11}\mathbf{s}^{n;1}_{21}, \tag{4a}$$

$$\mathbf{s}^{n;2}_{12} = \mathbf{s}^{n;1}_{12}[\mathbf{I} - \mathbf{S}^{n+1}_{11}\mathbf{s}^{n;1}_{22}]^{-1}\mathbf{S}^{n+1}_{12}, \tag{4b}$$

$$\mathbf{s}^{n;2}_{21} = \mathbf{S}^{n+1}_{21}[\mathbf{I} - \mathbf{s}^{n;1}_{22}\mathbf{S}^{n+1}_{11}]^{-1}\mathbf{s}^{n;1}_{21}, \tag{4c}$$

$$\mathbf{s}^{n;2}_{22} = \mathbf{S}^{n+1}_{22} + \mathbf{S}^{n+1}_{21}\mathbf{s}^{n;1}_{22}[\mathbf{I} - \mathbf{S}^{n+1}_{11}\mathbf{s}^{n;1}_{22}]^{-1}\mathbf{S}^{n+1}_{12}. \tag{4d}$$

Equations (4a)–(4d) stand for the GTSM of a two-box stack containing two interfaces but involving three layers. Now, we extend the definition in Eq. (2) to a stack containing $m \geq 2$ boxes by writing down

$$\begin{bmatrix} \mathbf{y}_{In}^{-} \\ \mathbf{y}_{Dn+m}^{-} \end{bmatrix} \equiv \begin{bmatrix} \mathbf{s}_{11}^{n;m} & \mathbf{s}_{12}^{n;m} \\ \mathbf{s}_{21}^{n;m} & \mathbf{s}_{22}^{n;m} \end{bmatrix} \begin{bmatrix} \mathbf{y}_{Dn}^{-} \\ \mathbf{y}_{In+m}^{-} \end{bmatrix}, \quad m \geq 2. \tag{5}$$

The submatrices $\mathbf{s}_{ij}^{n;m}$ in Eq. (5) of $\mathbf{s}^{n;m}$—the GTSM of the m-box stack—are obtained from Eqs. (4a)–(4d) by substituting $(n+1)$ with $(n+m)$ and $(n;2)$ with $(n;m)$, namely,

$$\mathbf{s}_{11}^{n;m} = \mathbf{s}_{11}^{n;m-1} + \mathbf{s}_{12}^{n;m-1}[\mathbf{I} - \mathbf{S}_{11}^{n+m}\mathbf{s}_{22}^{n;m-1}]^{-1}\mathbf{S}_{11}^{n+m}\mathbf{s}_{21}^{n;m-1}, \tag{6a}$$

$$\mathbf{s}_{12}^{n;m} = \mathbf{s}_{12}^{n;m-1}[\mathbf{I} - \mathbf{S}_{11}^{n+m}\mathbf{s}_{22}^{n;m-1}]^{-1}\mathbf{S}_{12}^{n+m}, \tag{6b}$$

$$\mathbf{s}_{21}^{n;m} = \mathbf{S}_{21}^{n+m}[\mathbf{I} - \mathbf{s}_{22}^{n;m-1}\mathbf{S}_{11}^{n+m}]^{-1}\mathbf{s}_{21}^{n;m-1}, \tag{6c}$$

$$\mathbf{s}_{22}^{n;m} = \mathbf{S}_{22}^{n+m} + \mathbf{S}_{21}^{n+m}\mathbf{s}_{22}^{n;m-1}[\mathbf{I} - \mathbf{S}_{11}^{n+m}\mathbf{s}_{22}^{n;m-1}]^{-1}\mathbf{S}_{12}^{n+m}. \tag{6d}$$

Results in Eqs. (6a)–(6d) represent the recursive algorithms in terms of the full **s**-matrix. This **s**-matrix formalism is the most general form and is directly introduced without any restriction neither on the nature of wave modes nor on the actual geometry of propagation media that the black box represents.

We now apply the above derived **s**-matrix formalisms to piezoelectric stacks of flat layers of infinite extent in the x_2-plane. We first express the GISM $\mathbf{S}^n$ defined in Eq. (1) in terms of the more fundamental electroacoustic properties of the component layers. The field variables and wave motions are represented by an eight-component state vector defined by $\boldsymbol{\tau}=[T_{21}T_{22}T_{23}D_2v_1v_2v_3\psi]^T$, which is formed by a linear combination of the basic eigensolutions ($\mathbf{Q}$ and $\mathbf{E}$) as follows, see Zhang *et al.*[20] for notations:

$$\boldsymbol{\tau}(x_1,x_2,t) = \mathbf{Q}\mathbf{y}(x_2)e^{i\omega(t-s_1x_1)}, \tag{7}$$

where $\mathbf{y}(x_2) \equiv \mathbf{E}(x_2)\tilde{\mathbf{y}}$ and $\mathbf{E}(x_2) \equiv e^{-i\omega\mathbf{s}_2x_2}$. Here, $\tilde{\mathbf{y}}$ is the mode amplitude vector associated with the eigensolutions $\mathbf{Q}$, and $\mathbf{s}_2$ is the diagonal spectral matrix. $\tilde{\mathbf{y}}$, $\mathbf{s}_2$, and $\mathbf{Q}$ vary from layer to layer but are keep constant within a given layer. $\mathbf{y}(x_2)$ is the position-dependent amplitudes; in particular it takes on values of $\mathbf{y}^{\mp}$ at the layer's top (−) and bottom (+) surface. The partial or eigenmodes are arranged as usual, i.e., $\mathbf{Q}^D=Q(:,1:4)$ for D-modes and $\mathbf{Q}^I=Q(:,5:8)$ for I-modes. Herein the MATLAB notations are employed for denoting the elements of a matrix, as explained in Ref. 20. We introduce now an *interface scattering matrix*, $\mathbf{R}_n$ for the interface separating two adjacent layers n and $n+1$, already used for simpler seismic waves.[11] We define $\mathbf{R}_n$ by

$$\begin{bmatrix} \mathbf{y}_{In}^{+} \\ \mathbf{y}_{Dn+1}^{-} \end{bmatrix} \equiv [\mathbf{R}_n] \begin{bmatrix} \mathbf{y}_{Dn}^{+} \\ \mathbf{y}_{\mathrm{In+1}}^{-} \end{bmatrix}. \tag{8}$$

Using the relations $\boldsymbol{\tau}_n^{+} \equiv \mathbf{Q}_n^D\mathbf{y}_{Dn}^{+} + \mathbf{Q}_n^I\mathbf{y}_{In}^{+}$ and $\boldsymbol{\tau}_{n+1}^{-} \equiv \mathbf{Q}_{n+1}^D\mathbf{y}_{Dn+1}^{-} + \mathbf{Q}_{n+1}^I\mathbf{y}_{In+1}^{-}$ yielded from Eq. (7) along with the state vector continuity $\boldsymbol{\tau}_n^{+} = \boldsymbol{\tau}_{n+1}^{-}$, we derive from Eq. (8) an expression of $\mathbf{R}_n$ in terms of the modal matrices of both layers,

$$\mathbf{R}_n = -[\mathbf{Q}_n^I - \mathbf{Q}_{n+1}^D]^{-1}[\mathbf{Q}_n^D - \mathbf{Q}_{n+1}^I]. \tag{9}$$

We underline that $\mathbf{R}_n$ depends on the electroacoustic properties of both layers surrounding the interface n but is independent of their thickness. Further, the $\mathbf{R}_n$ matrix as expressed in the complete form Eq. (9) fails for a singular matrix $[\mathbf{Q}_n^I - \mathbf{Q}_{n+1}^D]$. This happens, for example, for an interface separating a solid and a vacuum. Therefore, it is useful in some situations to have at one's disposal the submatrices of $\mathbf{R}_n$. We have derived them explicitly as follows:

$$\mathbf{R}_n^{11} = \mathbf{C}^{-1}(\mathbf{G}_n^D - \mathbf{G}_{n+1}^D), \tag{10a}$$

$$\mathbf{R}_n^{12} = \mathbf{C}^{-1}(\mathbf{G}_{n+1}^D - \mathbf{G}_{n+1}^I), \tag{10b}$$

$$\mathbf{R}_n^{21} = \mathbf{C}^{-1}(\mathbf{G}_n^D - \mathbf{G}_n^I), \tag{10c}$$

$$\mathbf{R}_n^{22} = \mathbf{C}^{-1}(\mathbf{G}_n^I - \mathbf{G}_{n+1}^I). \tag{10d}$$

Above, $\mathbf{C} \equiv \mathbf{G}_{n+1}^D - \mathbf{G}_n^I$, the symbol $\mathbf{G}_n^x$ is defined by $\mathbf{G}_n^x \equiv \mathbf{t}_n^x(\mathbf{v}_n^x)^{-1}$ $(x=D, I)$, with $\mathbf{t}_n^D \equiv \mathbf{Q}_n^{11}$, $\mathbf{t}_n^I \equiv \mathbf{Q}_n^{12}$, $\mathbf{v}_n^D \equiv \mathbf{Q}_n^{21}$, and $\mathbf{v}_n^I \equiv \mathbf{Q}_n^{22}$. $\mathbf{Q}_n^{ij}$ denote submatrices of $\mathbf{Q}_n$. $\mathbf{G}_n^x$ is nothing but the *characteristic surface impedance matrices* (CSIM) of a half space of the same material as the layer n. The term *characteristic* here expresses the fact that $\mathbf{G}_n^x$ depends only on the material properties of the layer n and is independent of fh (frequency or layer thickness). The diagonal and antidiagonal submatrices of $\mathbf{R}_n$ are what were called *local reflection and transmission matrices*, respectively.[11,15] $\mathbf{R}_n^{ij}$ exhibit poles when the matrix $\mathbf{C}$ becomes singular for certain s_1 values. This happens for SAW (surface acoustic wave) on the free surface of a semi infinite solid, and in some specific crystalline configurations where the interface wave is pertained. The amplitudes at both surfaces (±) of a layer are related by

$$\mathbf{y}_{Dn}^{+} = \mathbf{e}_n^D\mathbf{y}_{Dn}^{-} \quad \text{and} \quad \mathbf{y}_{In}^{-} = (\mathbf{e}_n^I)^{-1}\mathbf{y}_{In}^{+}, \tag{11}$$

with $\mathbf{e}^x \equiv \mathbf{v}^x e^{-j\omega s_2^x h}(\mathbf{v}^x)^{-1}$, $x=D,I$. $\mathbf{v}^D \equiv \mathbf{Q}(5:8,1:4)$, $\mathbf{v}^I \equiv \mathbf{Q}(5:8,5:8)$, $\mathbf{s}_2^D \equiv \mathbf{s}_2(1:4,1:4)$ and $\mathbf{s}_2^I \equiv \mathbf{s}_2(5:8,5:8)$, and h is the layer thickness, all of them refer to the layer n. Eliminating $\mathbf{y}_{xn}^{+}$ from Eqs. (8) and (11), we find again the relation (1), with the GISM $\mathbf{S}^n$ given by

$$\mathbf{S}^n = \begin{bmatrix} (\mathbf{e}_n^I)^{-1} & \mathbf{0} \\ \mathbf{0} & \mathbf{I} \end{bmatrix} [\mathbf{R}_n] \begin{bmatrix} \mathbf{e}_n^D & \mathbf{0} \\ \mathbf{0} & \mathbf{I} \end{bmatrix} = \begin{bmatrix} (\mathbf{e}_n^I)^{-1}\mathbf{R}_n^{11}\mathbf{e}_n^D & (\mathbf{e}_n^I)^{-1}\mathbf{R}_n^{12} \\ \mathbf{R}_n^{21}\mathbf{e}_n^D & \mathbf{R}_n^{22} \end{bmatrix}. \tag{12}$$

III. BC AND CHARACTERISTIC FUNCTIONS GIVING PROPER MODES

The recursive algorithm derived above applies to a stack of any number m of total layers with an arbitrary index n of the first layer. The reflection and transmission properties of a piezoelectric stack can thus be analyzed by means of the recursive algorithm [Eqs. (6a)–(6d) along with Eqs. (9), (10a)–(10d), and (12). The proper modes depend on both the stack and the surrounding media. An external surface of the stack can be stress-free or clamped for mechanical variables, and metallized or not for electrical variables. The stack BC must belong to some combinations of the mentioned conditions. In a general and versatile way, any BC can be expressed in terms of a *generalized surface impedance matrix* (GSIM)—$\mathbf{G}_{\mathrm{ex}}$ for the surface of either external media in contact with the stack. To be definitive, we assume from now on that all layers of finite thickness are contained in the stack and, consequently, on either side of the stack can only exist a

half space which is allowed to be a vacuum or a piezoelectric solid. With this in mind, the unique configuration that we have to consider is a finite-thick stack sandwiched in between two homogeneous half spaces. Let the stack layers be numbered from $n=1$ to $N\geq 2$, which implies that in Eqs. (5) and (6a)–(6d) $m=N-1$, and that the top and bottom half spaces are numbered with 0 and $N+1$. Their GSIM, becoming CSIM in this case, are still denoted by $\mathbf{G}_{\mathrm{ex}}^{-}$ and $\mathbf{G}_{\mathrm{ex}}^{+}$, respectively. Applying the state vector continuity at both interfaces separating the stack and the external media yields a global system with all four amplitudes vectors kept,

$$\begin{bmatrix} \mathbf{s}_{11}^{1;N-1} & -\mathbf{I} & \mathbf{0} & \mathbf{s}_{12}^{1;N-1}(\mathbf{e}_N^I)^{-1} \\ \mathbf{s}_{21}^{1;N-1} & \mathbf{0} & -\mathbf{I} & \mathbf{s}_{22}^{1;N-1}(\mathbf{e}_N^I)^{-1} \\ \mathbf{G}_{\mathrm{ex}}^{-}-\mathbf{G}_1^D & \mathbf{G}_{\mathrm{ex}}^{-}-\mathbf{G}_1^I & \mathbf{0} & \mathbf{0} \\ \mathbf{0} & \mathbf{0} & (\mathbf{G}_N^D-\mathbf{G}_{\mathrm{ex}}^{+})\mathbf{e}_N^D & \mathbf{G}_N^I-\mathbf{G}_{\mathrm{ex}}^{+} \end{bmatrix} \times \begin{bmatrix} \mathbf{y}_{D1}^{-} \\ \mathbf{y}_{I1}^{-} \\ \mathbf{y}_{DN}^{-} \\ \mathbf{y}_{IN}^{+} \end{bmatrix} = \mathbf{0}(16x1). \tag{13}$$

In Eq. (13), we have considered $\mathbf{y}_{DN}^{-}$ instead of $\mathbf{y}_{DN}^{+}$ as an unknown in order to avoid potential overflow with $fh_N\rightarrow\infty$, which would occur if the factor $(\mathbf{e}_N^D)^{-1}$ instead of $\mathbf{e}_N^D$ was present within the system matrix. Nontrivial solutions require the system determinant Δ_{12}, also called *characteristic function*, to vanish. The zeros define the allowed values for the ω-k pair or the proper mode solutions. Once the proper modes are determined, all other wave features can be easily analyzed straightforwardly. In particular, the mode amplitudes can be determined from Eq. (13) for any specific ω-k pair, and the dispersion relation, say ω as a function of $k_1 \equiv s_1\omega$, yields as k_1 varies in a desired range. We limit our paper only to formulating the characteristic functions that give proper modes without dealing with other wave characteristics.

The final system giving rise to the characteristic function, as we formulated in the form of Eq. (13), has features of both flexibility and versatility: the effects on the wave spectra due to the stack itself and those due to the surrounding media are explicitly distinguished. The former is described by the total **s**-matrix $\mathbf{s}^{1;N-1}$, the latter is incorporated into two parametric matrices $\mathbf{G}_{\mathrm{ex}}^{\pm}$. Various BCs at both sides of the stack are thus allowed to be specified by the user and to be formulated in a way totally independent of the **s**-matrix recursion. This way, the **s**-matrix recursion is conducted once for all BCs the stack may be subjected to. This radically differs from the **R** or any partial matrix recursion schemes, which inherently require repeating the **s**-matrix recursions whenever the BCs at the starting side are modified. We now discuss briefly the relations between the GSIM $\mathbf{G}_{\mathrm{ex}}^{\pm}$ and the half space-related stack BC. Because all finite-thickness layers are by assumption included in the stack itself, an external medium must be a homogeneous half space, and is totally characterized by its CSIM, no matter whether it is a solid or a vacuum. If the stack bottom is a solid, one has $\mathbf{G}_{\mathrm{ex}}^{+}=\mathbf{G}_{N+1}^D$; if the stack top is a solid, then $\mathbf{G}_{\mathrm{ex}}^{-}=\mathbf{G}_0^I$, according to the definition of $\mathbf{G}_n^x$ after Eq. (9). If the top surface of the stack is nonmetallized and stress-free, equivalent to a vacuum on the stack top, then $\mathbf{G}_{\mathrm{ex}}^{-}=\mathbf{G}_v$. $\mathbf{G}_v$ is a four-dimensional null matrix except for the (4,4)-element, which equals $j|s_1|\varepsilon_0$ and amounts to the vacuum contribution to the electrical variables. Finally, if the stack bottom is a vacuum, one has $\mathbf{G}_{\mathrm{ex}}^{+}=-\mathbf{G}_v$. The case of a metallized surface can be deduced from the above results by letting ε_0 tend to the infinity. The mechanically clamped surface BCs are not detailed here for the reason that they are difficult to realize in practice. As a matter of fact, using two GSIM $\mathbf{G}_{\mathrm{ex}}^{\pm}$ to represent external effects is a versatile way of expressing the stack BC. This remains true and so the resultant system [Eq. (13)] still applies even if the surrounding media are layered instead of homogeneous half spaces. Of course, $\mathbf{G}_{\mathrm{ex}}^{\pm}$ appearing in Eq. (13) should be specified accordingly, which is beyond the scope of the current paper.

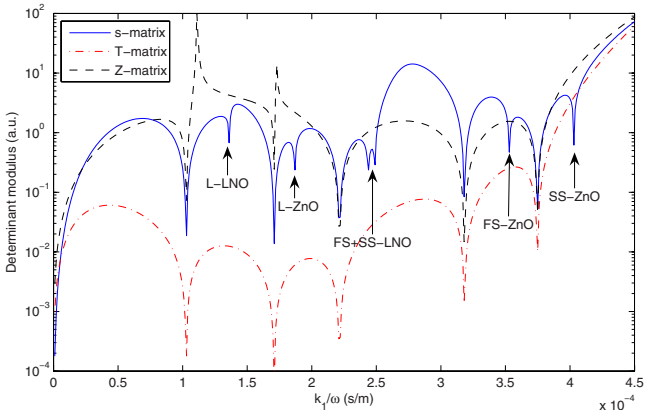

FIG. 2. (Color online) Characteristic functions given by three different formalisms for a bilayer (10,20,30)-ZnO/LiNbO$_3$ with $h_{1,2}=h=1$ μm, $fh=1000$ m/s. In addition to the five dips (true zeros for plate modes) common to the three curves, the **s**-matrix shows six dips due to pseudozeros (SSBW), as indicated by arrows for three SSBW of ZnO at $s_1=4.03$, 3.53, and 1.87, and three SSBW of LiNbO$_3$ at $s_1=2.49$, 2.44, and 1.36 (10^{-4} s/m), and the **Z**-matrix shows two peaks (poles).

IV. NUMERICAL FEATURES OF THE FULL S-MATRIX FORMALISM

Below, we illustrate numerical features of the full **s**-matrix formalism by considering a bilayer ZnO/LiNbO$_3$ plate of arbitrary crystalline orientation. Both surfaces are assumed to be stress-free and nonmetallized. The individual layer thickness was assumed to be $h=1$ μm in all examples. The characteristic functions are plotted against the parallel slowness $s_1\equiv k_1/\omega$ for some fixed values of fh. A curve dip shows either a true or a pseudozero of the function. Figure 2 shows for a moderate $fh=1000$ m/s the results for the **s**-matrix, along with the **Z** and **T** matrix results for comparison. Five true zeros are present which are common to all three curves and due to *plate modes* or generalized Lamb modes. The six additional dips of the **s**-matrix curve are pseudozeros and are related to the so-called *surface skimming bulk waves* (SSBW), three in each material. SSBW appear for some particular values of s_1, the so-called branch points at which the eigenvalue s_2 is double-valued but not necessarily zero. Although all of the three curves show the

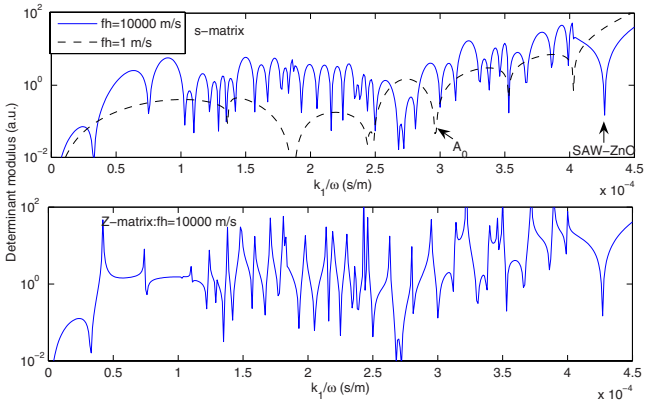

FIG. 3. (Color online) Characteristic functions of the same bilayer as in Fig. 2. Upper panel given by **s**-matrix: only A_0–like plate mode exists along with six SSBW for $fh=1$ m/s; A_0–like mode becomes a SAW-like in ZnO material, indicated by an arrow, along with a lot of higher order plate modes (dips) for $fh=10000$ m/s; Lower panel given by **Z**-matrix: many poles are mixed with zeros for $fh=10000$ m/**s**.

same plate modes, only the **s**-matrix is sensitive to SSBW. Some poles are present with the **Z**-matrix but not with the **T**- or the **s**-matrix. For this relatively low fh value, the superiority of the **s**-matrix over the **T**- or **Z**-matrix is not obvious since the stability issue is not involved and a few poles do not bother much the observation of zeros. With increasing fh, the number of plate modes increases and the basic (A_0-like) plate mode tends to the SAW in the slow ZnO layer, which behaves like a half space at sufficiently high $fh=10\,000$ m/s, as indicated in the top panel of Fig. 3. The **T**-matrix curve is not presentable and is so not presented due to the numerical instability at this relatively high fh. As to the **Z**-matrix, though the result remains stable, the function curve exhibits a lot of poles, as shown in the lower panel of Fig. 3. The presence of poles makes it difficult to observe on the graphs and to numerically locate the zeros which are hidden among the poles when the modes are dense at very high frequencies. At an extremely low $fh=1$ m/s, on the other hand, only one plate (A_0-like) mode exists in addition to the six pseudozeros due to SSBW, and the **s**-matrix remains stable, see the upper panel of Fig. 3, as contrasted to the **Z**-matrix one which becomes unstable.[15]

To go further, we tested the **s**-matrix formalism for fh as high as $fh=100\,000$ m/s. In the spectral range shown in Fig. 4, 4500 uniform samplings were sufficient to clearly distinguish all of the 310 dips (complete set of modes). No bad matrix condition was reported by MATLAB during calculations. The proper modes are so many and so dense that the full spectra become difficult to be numerically determined with other formalisms, either due to loss of precision (**T**-matrix) or impossibility of distinguishing mixed zeros and poles (**Z**-matrix) with a reasonable number of sampling points. Referring to the lower panel of Fig. 3, it is not hard to figure out how the **Z**-matrix curve might look when about ten times more poles and zeros mix together. The characteristic function we formulated using the **s**-matrix is not only stable like the **Z**- or **K**-matrix, but also exhibits nice functional features: being pole-free in contrast to the **Z**-matrix, and keeping a rather steady magnitude over the entire range of k_1 in contrast to the **T**-matrix whose curve, as seen in Figs. 2, will grows rapidly with high fh and for sufficiently high k_1 values even in stable regimes. We also applied the full **s**-matrix formalism to a three-layer ZnO/LNO/ZnO plate with the same BC as before. The obtained results, not presented here, are similar to those for the bilayer except for the absence of the dips related to the SSBW modes of the LNO material though the three dips due to the SSBW of ZnO were

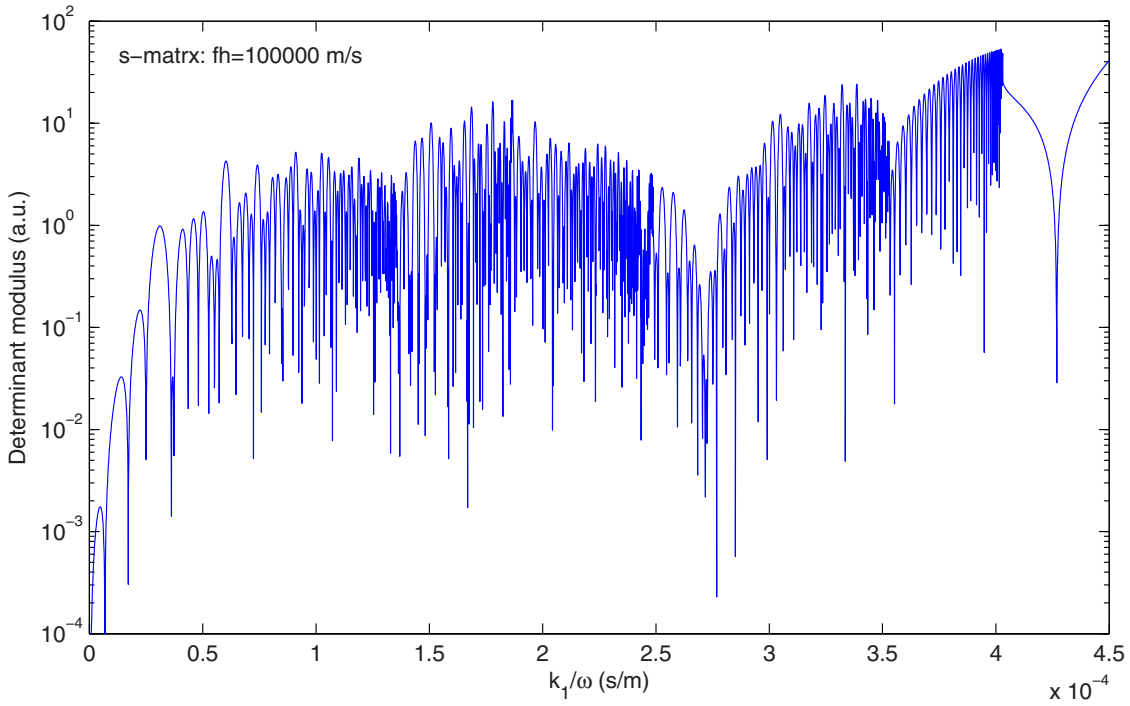

FIG. 4. (Color online) Characteristic function of the same bilayer as in Fig. 2 given by **s**-matrix for $fh=100000$ m/s with 4500 uniform samplings used in the shown k_1-range. A total of 310 modes (curve dips) are present and all are well distinguishable with the graph magnified. The right-most dip is the SAW of ZnO, a less remarkable dip at 2.718 is the SAW of $LiNbO_3$. Other 308 dips are plate modes along with the 6 SSBW.

still present. We explain this phenomenon by noting that the wave amplitudes of the middle LNO layer do not appear in Eq. (13) leading to the characteristic function Δ_{12}. The same three-layer plate terminated on an additional LNO half space was investigated as well. Again, the three SSBW of ZnO were observed but the SSBW of LNO were not. Instead, some pseudo-SAW appeared near the SSBW of LNO and they become more and more visible as fh decreases.

V. COMMENTS AND CONCLUSIONS

A comprehensive approach for the modeling of acoustic waves in stacked piezoelectric structures is presented based on the stack's total scattering matrix. Instead of elevating the **s**-matrix algorithms from quarter- or half-matrix recursions, we derived them directly from the basic physical definition of the **s**-matrix. As a consequence, our recursion scheme is concise and unified. It naturally incorporates within a single **s**-matrix the stack reflection and transmission matrices of both the input and output sides. The full **s**-matrix recursion can be conducted for a given stack regardless of the surrounding media. Thus it obviates the need to preliminarily specify the BC on one side of the stack and then to proceed the recursion toward the other side as with the **R**-matrix.[12] Without the need of incorporating the BC into the recursions at the outset, the same **s**-matrix recursion results remain valid and applicable for studying proper modes associated with various BCs.

Compared with other matrix formalisms, the **s**-matrix exhibits superior properties considering all of the criteria: asymptotic behaviors as the frequency tends to zero or infinity, absence of poles, and the sensitivity to SSBW, as well as being dimensionless, as summarized in Table I. It gives the pole-free characteristic functions, such as the **T**-matrix; but it is unconditionally stable throughout large and small thicknesses, such the **H**-matrix. The piezoelectric **Z**-matrix formalism, though also unconditionally stable, possesses poles which might be troubling in numerical calculations. In addition to its instability at low fh, the existence of intrinsic poles is in our opinion a major drawback of the **Z**-matrix formalism. The **K**-matrix, a direct variant of the **Z**-matrix, should have exactly the same properties as **Z**, and so is expected to possess poles for piezoelectric materials. A certain physical signification can be attributed to the poles, which generally correspond to proper modes associated with some exotic BCs that have no obvious practical interests. The full **s**-matrix recursion we presented here is the only formalism that is both pole-free and unconditionally stable. The **s**-matrix involves only homogeneous matrix elements such as **Z** or **K** matrix; this property was claimed to be more desirable than the heterogeneous **T** and **H** matrices.[15] Better, it is the only one involving dimensionless matrix elements, which naturally facilitates the numerical normalization. The **s**-matrix-based characteristic function, such as $\Delta_{12}(\omega, s_1)$ considering the mode amplitudes, is independent of the arbitrary eigenvectors norm in the **Q**-matrix and has a definitive phase. A stable sign of the function with the iterative variable s_1 is indispensable for implementing numerical zero-finding algorithms based on the sign-detection scheme.

Our total **s**-matrix formalism is numerically more efficient than partial matrix recursions because the proper modes associated with several sets of BC can be determined in parallel by performing a single **s**-matrix recursion. The computational gain is especially significant when different BCs are to be considered for a stack containing a lot of layers. For a stack beginning with a half space, computation efficiency of the full **s**-matrix formalism can still be improved by performing a quarter-matrix recursion, i.e., the (2,2)-element $\mathbf{s}_{22}$ alone is recursively determined without calculating all other submatrices of **s**. This is possible because $\mathbf{s}_{22}^{1;N-1}$ of the final stack depends only on the (2,2)-element $\mathbf{s}_{22}^{1;N-2}$ of the previous stack [see Eq. (6d)], and $\mathbf{s}_{22}^{1;N-1}$ is the only needed submatrix of $\mathbf{s}^{1;N-1}$ with $\mathbf{y}_{D1}^{-}=\mathbf{0}$ in Eq. (13). When the beginning half space is a vacuum, however, some poles are introduced into the final characteristic function.

A peculiar feature of the **s**-matrix formalism resides in its high sensitivity to SSBW modes that are usually absent from the **Z**−, **K**-, and **T**-matrix formalisms. How about the **H**-matrix as regards the sensitivity to SSBW modes and possessing intrinsic poles or not, the answer is not yet widely known and would need further investigations. The presence of pseudozeros might be inconvenient if the numerical root finding scheme for true zeros is based on the local minima localization. However, pseudozeros have no harmful effect on the sign-detection algorithm, which is much more robust and reliable than the previous one. Since leaky SAW usually exists in close proximity to SSBW, the sensitivity to SSBW of the **s**-matrix is expected to find interest in establishing algorithms for leaky modes location. A thorough study is required in order to be able to explain in clear and simple physical terms the fundamental reason as to why the **s**-matrix is sensitive to the SSBW modes.

[1] A. H. Fahmy and E. L. Adler, Appl. Phys. Lett. **22**, 495 (1973).
[2] E. L. Adler, IEEE Trans. Ultrason. Ferroelectr. Freq. Control **37**, 485 (1990).
[3] M. J. S. Lowe, IEEE Trans. Ultrason. Ferroelectr. Freq. Control **42**, 525 (1995).
[4] E. L. Tan, J. Acoust. Soc. Am. **119**, 45 (2006).
[5] B. Honein, A. M. B. Braga, P. Barbone, and G. Herrmann, Proceedings of the Conference on Recent Advances in Active Control of Sound and Vibration, 1991 (unpublished), p. 50.
[6] B. Hosten and M. Castaings, Ultrasonics **41**, 501 (2003).
[7] B. Collet, Ultrasonics **42**, 189 (2004).
[8] S. I. Rokhlin and L. Wang, J. Acoust. Soc. Am. **112**, 822 (2002).
[9] L. Wang and S. I. Rokhlin, IEEE Trans. Ultrason. Ferroelectr. Freq. Control **51**, 453 (2004).
[10] B. L. N. Kennett, *Seismic Wave Propagation in Stratified Media* (Cambridge University Press, Cambridge, England, 1983).
[11] G. J. Fryer and L. N. Frazer, Geophys. J. R. Astron. Soc. **78**, 691 (1984).
[12] T. Pastureaud, V. Laude, and S. Ballandras, Appl. Phys. Lett. **80**, 2544 (2002).
[13] E. L. Tan, Ultrasonics **41**, 229 (2003).
[14] D. C. Booth and S. Crampin, Geophys. J. R. Astron. Soc. **72**, 755 (1983).
[15] E. L. Tan, IEEE Trans. Ultrason. Ferroelectr. Freq. Control **54**, 2016 (2007).
[16] R. Ludwig and P. Bretchko, *RF Circuit Design: Theory and Applications* (Prentice-Hall, Upper Saddle River, NJ, 2000).
[17] D. Y. K. Ko and J. R. Sambles, J. Opt. Soc. Am. A **5**, 1863 (1988).
[18] D. Y. K. Ko and J. C. Inkson, Phys. Rev. B **38**, 9945 (1988).
[19] A. Reinhardt, V. Laude, A. Khelif, and S. Ballandras, IEEE Trans. Ultrason. Ferroelectr. Freq. Control **51**, 1157 (2004).
[20] V. Y. Zhang, J.-E. Lefebvre, C. Bruneel, and T. Gryba, IEEE Trans. Ultrason. Ferroelectr. Freq. Control **48**, 1449 (2001).